

# Triple-Diffusive Natural Convection in a Square Porous Cavity

Mehdi Ghalambaz<sup>1</sup> · Faramarz Moattar<sup>2</sup> ·  
Mikhail A. Sheremet<sup>3,4</sup> · Ioan Pop<sup>5</sup>

Received: 17 July 2015 / Accepted: 22 September 2015 / Published online: 3 October 2015  
© Springer Science+Business Media Dordrecht 2015

**Abstract** The triple-diffusive flow, heat and mass transfer in a cavity filled with a porous medium and saturated with a mixture is theoretically studied in a cavity with differential temperature and concentrations at the side walls. The effect of buoyancy forces due to mass transfer of phases is also taken into account using the Boussinesq approximation. The governing equations are transformed into a non-dimensional form and numerically solved using the finite element method. Five groups of non-dimensional parameters including the Rayleigh number, the Lewis numbers for phases 1 and 2, and the buoyancy ratio parameters for phases 1 and 2 are obtained. The effect of each group of non-dimensional parameters on the heat and mass transfer in the cavity is discussed. The results show that for specific values of the Lewis number of one phase, the heat transfer of the mixture and the mass transfer of the other phase can be maximum. The presence of one phase could reduce or enhance the mass transfer of the second phase depending on the Lewis number of phases.

**Keywords** Triple diffusion · Natural convection · Porous media · Numerical analysis · Finite element method

---

✉ Mehdi Ghalambaz  
ghalambaz.mehdi@gmail.com

<sup>1</sup> Department of Environmental Engineering, Ahvaz Branch, Islamic Azad University, Ahvaz, Iran

<sup>2</sup> Department of Environmental Engineering, Graduate School of the Environment and Energy, Science and Research Branch, Islamic Azad University, Tehran, Iran

<sup>3</sup> Department of Theoretical Mechanics, Faculty of Mechanics and Mathematics, Tomsk State University, Tomsk, Russia 634050

<sup>4</sup> Institute of Power Engineering, Tomsk Polytechnic University, Tomsk, Russia 634050

<sup>5</sup> Department of Applied Mathematics, Babeş-Bolyai University, 400084 Cluj-Napoca, Romania

## 1 Introduction

The natural convection occurs due to buoyancy difference in a fluid. The well-known buoyancy force in fluids is the thermal expansion of the fluid. This effect has been extensively studied in the literature (Ingham and Pop 2005). There are also cases in which the natural convection is due to mass transfer in binary fluids. The migration of heavy molecules in a fluid could induce a buoyancy force in the fluid and result in a natural convection flow, which is known as double-diffusive convection. The simultaneous presence of concentration gradients and thermal differences in an enclosure could result in opposing or aided convective flows that in most case are very complicated in nature. The natural convective heat transfer of double-diffusive fluids inside porous media has been studied in many of previous publications, for example the study of Costa (2004), Varol et al. (2008), Chamkha and Al-Mudhaf (2008), Mahdy et al. (2010), Chamkha et al. (2010, 2011), Subhashini et al. (2011), Abdou and Chamkha (2012), Ravikumar et al. (2013) and Mallikarjuna et al. (2014). However, there are engineering applications in which the fluid consists of three phases with distinct densities and mass diffusive coefficients, for example the migration of moisture and natural gas through the air in soil or grains. The dispersion of chemical contaminants through water in saturated soil or dispersion of carbon dioxide and carbon monoxide through the air in natural convection in a fibrous media or filter.

Despite the many practical engineering applications of triple-diffusive natural convection heat and mass transfer in enclosures, the available studies in the literature are very limited. Rudraiah and Vortmeyer (1982), Poulikakos (1985), Kantur and Tsibulin (2004), Rionero (2012, 2013, 2014, 2015), Bulgarkova (2012), Capone and De Luca (2012) and Chand (2012, 2013) have addressed different aspects of the onset of instability in triple-diffusive convection in porous media. Khan et al. (2013, 2015) and Khan and Pop (2013) have analyzed the boundary layer heat and mass transfer of a three- component solution over a flat plate embedded in a porous media.

The present study aims to analyze the aided flow of triple-diffusive natural convective heat and mass transfer in an enclosure filled with a porous medium.

## 2 Basic Equations

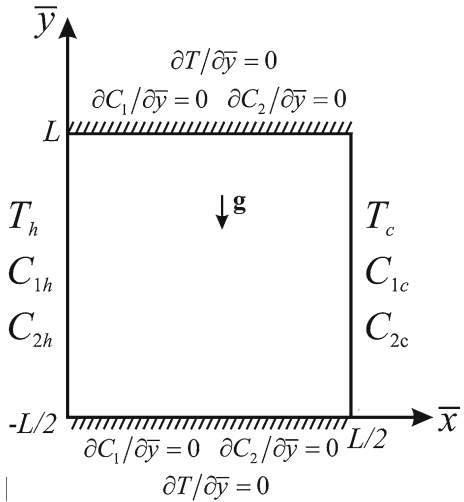
We consider the steady triple-diffusive convective flow in a square cavity filled with a fluid-saturated porous medium. A schematic geometry of the problem under investigation is shown in Fig. 1, where  $\bar{x}$  and  $\bar{y}$  are the Cartesian coordinates measured along the lower wall and along the vertical wall of the cavity, respectively, and  $L$  is the size of the cavity. The cavity is assumed to be impermeable, and the left vertical wall is maintained at the constant temperature  $T_h$  and concentrations  $C_{1h}$  and  $C_{2h}$ , while the right wall is maintained at the constant temperature  $T_c$  and concentrations  $C_{1c}$  and  $C_{2c}$ , respectively. The horizontal walls are adiabatic ( $\partial T / \partial \bar{y} = 0$ ) and impermeable ( $\partial C_1 / \partial \bar{y} = 0$  and  $\partial C_2 / \partial \bar{y} = 0$ ).

Following Rionero (2013), we also assume that two different chemical components (“salts”)  $S_m$  ( $m = 1, 2$ ) have dissolved in the fluid-saturated porous medium, which have concentrations  $C_m$  ( $m = 1, 2$ ), respectively, and that the equation of state is

$$\rho = \rho_0 [1 - \beta_T (T - T_0) - \beta_1 (C_1 - C_{1c}) - \beta_2 (C_2 - C_{2c})], \quad (1)$$

where  $\rho_0$  is a reference density and the constants  $\beta_T$ ,  $\beta_1$  and  $\beta_2$  denote the coefficient of thermal expansion and solute  $S_m$  expansion coefficients, respectively ( $m = 1, 2$ ), which are defined by

**Fig. 1** Schematic diagram of coordinate system and physical model



$$\beta_T = -\frac{1}{\rho} \left( \frac{\partial \rho}{\partial T} \right)_p, \quad \beta_1 = -\frac{1}{\rho} \left( \frac{\partial \rho}{\partial C_1} \right)_p, \quad \beta_2 = -\frac{1}{\rho} \left( \frac{\partial \rho}{\partial C_2} \right)_p. \tag{2}$$

Combining Darcy’s law

$$\frac{\mu}{K} \bar{\mathbf{v}} = -\nabla \bar{p} + \rho \mathbf{g}, \tag{3}$$

with (thermal) energy and continuity equations together with the Boussinesq approximation (1), we obtain the following fundamental vectorial equations in dimensional form governing the isochoric motions

$$\nabla \cdot \bar{\mathbf{v}} = 0, \tag{4}$$

$$\frac{\mu}{K} \bar{\mathbf{v}} = -\nabla \bar{p} + \rho_0 [1 - \beta_T (T - T_0) - \beta_1 (C_1 - C_C) - \beta_2 (C_2 - C_C)] \mathbf{g}, \tag{5}$$

$$\bar{\mathbf{v}} \cdot \nabla T = \alpha_m \nabla^2 T, \tag{6}$$

$$\frac{1}{\varepsilon} \bar{\mathbf{v}} \cdot \nabla C_1 = D_1 \nabla^2 C_1, \tag{7}$$

$$\frac{1}{\varepsilon} \bar{\mathbf{v}} \cdot \nabla C_2 = D_2 \nabla^2 C_2, \tag{8}$$

where  $\bar{\mathbf{v}}$  is the velocity vector,  $\bar{p}$  is the pressure field,  $\mu$  is the dynamic viscosity,  $K$  is the permeability,  $\mathbf{g}$  is the gravity vector,  $\alpha_m$  is the thermal diffusivity of the porous medium and  $D_m$  ( $m = 1, 2$ ) are the mass diffusivity of the salts  $S_m$ .

Eliminating the pressure  $\bar{p}$  from Eq. (5), the following governing equations for the proposed model are valid in Cartesian coordinates  $\bar{x}$  and  $\bar{y}$

$$\frac{\partial \bar{u}}{\partial \bar{x}} + \frac{\partial \bar{v}}{\partial \bar{y}} = 0, \tag{9}$$

$$\frac{\partial \bar{u}}{\partial \bar{y}} - \frac{\partial \bar{v}}{\partial \bar{x}} = -\frac{gK}{\mu} \left( \beta_T \frac{\partial T}{\partial \bar{x}} + \beta_1 \frac{\partial C_1}{\partial \bar{x}} + \beta_2 \frac{\partial C_2}{\partial \bar{x}} \right) \tag{10}$$

$$\bar{u} \frac{\partial T}{\partial \bar{x}} + \bar{v} \frac{\partial T}{\partial \bar{y}} = \alpha_m \left( \frac{\partial^2 T}{\partial \bar{x}^2} + \frac{\partial^2 T}{\partial \bar{y}^2} \right), \tag{11}$$

$$\frac{1}{\varepsilon} \left( \bar{u} \frac{\partial C_1}{\partial \bar{x}} + \bar{v} \frac{\partial C_1}{\partial \bar{y}} \right) = D_1 \left( \frac{\partial^2 C_1}{\partial \bar{x}^2} + \frac{\partial^2 C_1}{\partial \bar{y}^2} \right), \quad (12)$$

$$\frac{1}{\varepsilon} \left( \bar{u} \frac{\partial C_2}{\partial \bar{x}} + \bar{v} \frac{\partial C_2}{\partial \bar{y}} \right) = D_2 \left( \frac{\partial^2 C_2}{\partial \bar{x}^2} + \frac{\partial^2 C_2}{\partial \bar{y}^2} \right), \quad (13)$$

Further, we introduce the following dimensionless variables

$$\begin{aligned} x &= \bar{x}/L, & y &= \bar{y}/L, & u &= \bar{u}L/\alpha_m, & v &= \bar{v}L/\alpha_m, & \theta &= (T - T_0)/\Delta T \\ \phi_1 &= (C_1 - C_{1c})/\Delta C_1, & \phi_2 &= (C_2 - C_{2c})/\Delta C_2, \end{aligned} \quad (14)$$

where  $T_0 = (T_h + T_c)/2$  is the mean temperature of heated and cooled vertical walls of the cavity,  $\Delta T = T_h - T_c$ ,  $\Delta C_1 = C_{1h} - C_{1c}$  and  $\Delta C_2 = C_{2h} - C_{2c}$ .

Further, we introduce the dimensionless stream function  $\psi$  defined by

$$u = \frac{\partial \psi}{\partial y}, \quad v = -\frac{\partial \psi}{\partial x}, \quad (15)$$

such that the continuity Eq. (9) is automatically satisfied. We are then left with the following five equations,

$$\frac{\partial^2 \psi}{\partial x^2} + \frac{\partial^2 \psi}{\partial y^2} = -Ra \left( \frac{\partial \theta}{\partial x} + Nc_1 \frac{\partial \phi_1}{\partial x} + Nc_2 \frac{\partial \phi_2}{\partial x} \right), \quad (16)$$

$$\frac{\partial \psi}{\partial y} \frac{\partial \theta}{\partial x} - \frac{\partial \psi}{\partial x} \frac{\partial \theta}{\partial y} = \frac{\partial^2 \theta}{\partial x^2} + \frac{\partial^2 \theta}{\partial y^2}, \quad (17)$$

$$Le_1 \left( \frac{\partial \psi}{\partial y} \frac{\partial \phi_1}{\partial x} - \frac{\partial \psi}{\partial x} \frac{\partial \phi_1}{\partial y} \right) = \frac{\partial^2 \phi_1}{\partial x^2} + \frac{\partial^2 \phi_1}{\partial y^2}, \quad (18)$$

$$Le_2 \left( \frac{\partial \psi}{\partial y} \frac{\partial \phi_2}{\partial x} - \frac{\partial \psi}{\partial x} \frac{\partial \phi_2}{\partial y} \right) = \frac{\partial^2 \phi_2}{\partial x^2} + \frac{\partial^2 \phi_2}{\partial y^2}, \quad (19)$$

with the boundary conditions

$$\begin{aligned} \psi &= 0, & \theta &= 0.5, & \phi_1 &= 1, & \phi_2 &= 1 & \text{on } x &= -0.5 \\ \psi &= 0, & \theta &= -0.5, & \phi_1 &= 0, & \phi_2 &= 0 & \text{on } x &= 0.5 \\ \psi &= 0, & \frac{\partial \theta}{\partial y} &= 0, & \frac{\partial \phi_1}{\partial y} &= 0, & \frac{\partial \phi_2}{\partial y} &= 0 & \text{on } y &= 0 \text{ and } y = 1, \end{aligned} \quad (20)$$

where  $Ra$  is the Rayleigh number for the porous medium,  $Nc_1$  and  $Nc_2$  are the buoyancy parameters for the salts 1 and 2, and  $Le_1$  and  $Le_2$  are the Lewis numbers for the salts 1 and 2, which are defined

$$Ra = \frac{gK\beta_T\Delta TL}{\nu\alpha_m}, \quad Nc_1 = \frac{\beta_1\Delta C_1}{\beta_T\Delta T}, \quad Nc_2 = \frac{\beta_2\Delta C_2}{\beta_T\Delta T}, \quad Le_1 = \frac{\alpha_m}{\varepsilon D_1}, \quad Le_2 = \frac{\alpha_m}{\varepsilon D_2}, \quad (21)$$

The physical quantities of practical interest are the local Nusselt number  $Nu$  and the local Sherwood numbers  $Sh_1$  and  $Sh_2$  for salts 1 and 2, respectively, which are defined as

$$\begin{aligned} Nu &= \frac{L}{\Delta T} \left( -\frac{\partial T}{\partial \bar{x}} \right)_{\bar{x}=-0.5}, & Sh_1 &= \frac{L}{\Delta C_1} \left( -\frac{\partial C_1}{\partial \bar{x}} \right)_{\bar{x}=-0.5}, \\ Sh_2 &= \frac{L}{\Delta C_2} \left( -\frac{\partial C_2}{\partial \bar{x}} \right)_{\bar{x}=-0.5}. \end{aligned} \quad (22)$$

Substituting (14) into (22), we obtain

$$Nu = \left(-\frac{\partial\theta}{\partial x}\right)_{x=-0.5}, \quad Sh_1 = \left(-\frac{\partial\phi_1}{\partial x}\right)_{x=-0.5}, \quad Sh_2 = \left(-\frac{\partial\phi_2}{\partial x}\right)_{x=-0.5}. \quad (23)$$

Also, of interest are the average Nusselt number  $\overline{Nu}$  and average Sherwood numbers  $\overline{Sh}_1$  and  $\overline{Sh}_2$ , which are given by

$$\overline{Nu} = \int_0^1 Nu dy, \quad \overline{Sh}_1 = \int_0^1 Sh_1 dy, \quad \overline{Sh}_2 = \int_0^1 Sh_2 dy. \quad (24)$$

### 3 Numerical Method

The non-dimensional governing equations, represented by Eqs. (19)–(21), and subject to the boundary conditions, Eq. (20), were written in weak form and solved numerically utilizing Galerkin finite element method (Reddy 1993). Invoking basis set  $\{\xi_k\}_{k=1}^N$ , the stream function ( $\psi$ ), the temperature, the concentration for phase 1, and the concentration for phase 2 were expanded as,

$$\begin{aligned} \psi &\approx \sum_{k=1}^N \psi_k \xi_k(x, y), \quad \theta \approx \sum_{k=1}^N \theta_k \xi_k(x, y), \quad \phi_1 \approx \sum_{k=1}^N \phi_{1k} \xi_k(x, y), \\ \phi_2 &\approx \sum_{k=1}^N \phi_{2k} \xi_k(x, y), \end{aligned} \quad (25)$$

for  $-0.5 < x < 0.5$  and  $0 < y < 1$ . For all four variables, the basis function is the same, and hence, the total number of nodes for all variables is  $N$ . Employing the Galerkin finite element method on Eqs. (16)–(19) at nodes of internal domain  $\Omega$ , the nonlinear residual equations are, respectively, derived as,

$$\begin{aligned} R_i^1 &= \sum_{k=1}^N \psi_k \int_{\Omega} \left[ \frac{\partial \xi_i}{\partial x} \frac{\partial \xi_k}{\partial x} + \frac{\partial \xi_i}{\partial y} \frac{\partial \xi_k}{\partial y} \right] dx dy - Ra \left( \sum_{k=1}^N \theta_k \int_{\Omega} \frac{\partial \xi_k}{\partial x} \xi_i dx dy \right) \\ &\quad - Ra.Nc_1 \left( \sum_{k=1}^N \phi_{1k} \int_{\Omega} \frac{\partial \xi_k}{\partial x} \xi_i dx dy \right) - Ra.Nc_2 \left( \sum_{k=1}^N \phi_{2k} \int_{\Omega} \frac{\partial \xi_k}{\partial x} \xi_i dx dy \right), \end{aligned} \quad (26)$$

$$\begin{aligned} R_i^2 &= \left( \sum_{k=1}^N \psi_k \int_{\Omega} \frac{\partial \xi_k}{\partial y} \xi_i dx dy \right) \left( \sum_{k=1}^N \theta_k \int_{\Omega} \frac{\partial \xi_k}{\partial x} \xi_i dx dy \right) \\ &\quad - \left( \sum_{k=1}^N \psi_k \int_{\Omega} \frac{\partial \xi_k}{\partial x} \xi_i dx dy \right) \left( \sum_{k=1}^N \theta_k \int_{\Omega} \frac{\partial \xi_k}{\partial y} \xi_i dx dy \right) \\ &\quad + \sum_{k=1}^N \theta_k \int_{\Omega} \left( \frac{\partial \xi_i}{\partial x} \frac{\partial \xi_k}{\partial x} + \frac{\partial \xi_i}{\partial y} \frac{\partial \xi_k}{\partial y} \right), \end{aligned} \quad (27)$$

$$R_i^3 = Le_1 \left( \sum_{k=1}^N \psi_k \int_{\Omega} \frac{\partial \xi_k}{\partial y} \xi_i dx dy \right) \left( \sum_{k=1}^N \phi_{1k} \int_{\Omega} \frac{\partial \xi_k}{\partial x} \xi_i dx dy \right)$$

$$\begin{aligned}
& -Le_1 \left( \sum_{k=1}^N \psi_k \int_{\Omega} \frac{\partial \xi_k}{\partial x} \xi_i dx dy \right) \left( \sum_{k=1}^N \phi_{1k} \int_{\Omega} \frac{\partial \xi_k}{\partial y} \xi_i dx dy \right) \\
& + \sum_{k=1}^N \phi_{1k} \int_{\Omega} \left( \frac{\partial \xi_i}{\partial x} \frac{\partial \xi_k}{\partial x} + \frac{\partial \xi_i}{\partial y} \frac{\partial \xi_k}{\partial y} \right), \tag{28}
\end{aligned}$$

and

$$\begin{aligned}
R_i^4 & = Le_2 \left( \sum_{k=1}^N \psi_k \int_{\Omega} \frac{\partial \xi_k}{\partial y} \xi_i dx dy \right) \left( \sum_{k=1}^N \phi_{2k} \int_{\Omega} \frac{\partial \xi_k}{\partial x} \xi_i dx dy \right) \\
& - Le_2 \left( \sum_{k=1}^N \psi_k \int_{\Omega} \frac{\partial \xi_k}{\partial x} \xi_i dx dy \right) \left( \sum_{k=1}^N \phi_{2k} \int_{\Omega} \frac{\partial \xi_k}{\partial y} \xi_i dx dy \right) \\
& + \sum_{k=1}^N \phi_{2k} \int_{\Omega} \left( \frac{\partial \xi_i}{\partial x} \frac{\partial \xi_k}{\partial x} + \frac{\partial \xi_i}{\partial y} \frac{\partial \xi_k}{\partial y} \right). \tag{29}
\end{aligned}$$

In the above residual equations,  $R_i$ , the bi-quadratic functions with three-point Gaussian quadrature were utilized to evaluate the integrals. Moreover, the Newton–Raphson method is employed to solve the nonlinear residual equations, Eqs. (26)–(29), for the coefficients of the expansions in Eq. (25). The details of the solution procedure have been discussed in the literature (Reddy 1993; Basak et al. 2006a, b) and have not been repeated here for the sake of brevity. It should be noted that the model incorporates Darcy’s law and the Lewis numbers which could be large about order of 10. Therefore, the flow behavior next to the walls is very important. Hence, the discretized equations were implemented on the non-uniform grid. In the non-uniform grid, the grid points are symmetrically clustered near the walls in both  $x$  and  $y$  directions with the aspect ratio of 1.05. The obtained system of equations was solved iteratively. The iteration process commenced from the initial guess of zero for stream function and 0.5 for the temperature and concentrations and repeated until the residuals for the stream functions, temperature and concentrations become lower than  $10^{-7}$ . For parametric analysis of the problem, the parameter of study was smoothly increased and the obtained steady state solution in each step was utilized as an initial guess for the next solution in order to reduce the time of calculations. For example, for analysis of the effect of the increase in Rayleigh number on the solution, the problem was solved for  $Ra = 25$  and converged. Then, the obtained solution was utilized as an initial guess for  $Ra = 50$  and the iteration process commenced until the equations converge. The solution procedure, in the form of an in-house computational fluid dynamics (CFD) code, has been validated successfully against the results available in the literature.

### 3.1 Code Validation

In the case of a pure fluid when  $Nc_1 = Nc_2 = 0$ , a comparison between the results of the present study and the previous studies is performed in Table 1. Table 1 shows very good agreement between the results of the present study and those reported in the literature.

In addition, Costa (2004) has analyzed the double-diffusive natural convection in parallelogrammic enclosures filled with fluid-saturated porous media. Considering parallelogrammic enclosures with the inclination angle of zero, the geometry of the study of Costa (2004) reduces to the geometry of the present study, and assuming  $Nc_2 = Le_2 = 0$  the present study reduces to the problem of double-diffusive natural convection. Hence, in this case the

**Table 1** Comparison of the average Nusselt number of the hot wall

Authors	$Ra$		
	10	100	1000
Walker and Homsy (1978)		3.097	12.96
Beckermann et al. (1986)		3.113	
Gross et al. (1986)		3.141	13.448
Manole and Lage (1992)		3.118	13.637
Bejan (1979)		4.2	15.8
Baytas and Pop (1999)	1.079	3.16	14.06
Moya et al. (1987)	1.065	2.801	
Present results	1.08	3.11	13.64

**Table 2** Comparison of the average Nusselt number for the case of double-diffusive natural convection in a square cavity when  $Le_1 = 0.8$  and  $Nc_1 = 2$ 

Ref.	$Ra = 25$		$Ra = 50$		$Ra = 50$	
	$Nu$	$Sh_{1/Le_1}$	$Nu$	$Sh_{1/Le_1}$	$Nu$	$Sh_{1/Le_1}$
Costa (2004)	2.59	2.72	4.13	4.31	6.31	6.66
Present	2.61	2.74	4.18	4.35	6.62	6.93

results of the present study are validated against the results of Costa (2004) in Table 2. As seen, the results are in very good agreement.

### 3.2 Grid Check

A non-uniform structured  $100 \times 100$  mesh, expanding with a symmetric distribution from the walls toward the center of the cavity with the element ratio of 1.05, is selected after some experimental execution of the results. Table 2 shows the evaluated values of the Nusselt numbers for mixture and the Sherwood numbers for phases 1 and 2. The results are reported for different grid sizes and two values of Rayleigh numbers ( $Ra = 50$  and  $Ra = 100$ ) and three values of Lewis number phase 1 ( $Le_1 = 0.1, 1.0$  and  $10$ ) when  $Le_2 = 0.8$ ,  $Nc_1 = 2.0$  and  $Nc_2 = 2.0$ . Table 3 shows that the grid size of  $100 \times 100$  provides sufficient accuracy for the calculations. The results were also repeated for higher grid sizes, and consistence results were found. Hence, the grid size of  $100 \times 100$  was utilized for the calculations.

## 4 Results and Discussion

The non-dimensional parameters in the present study are the  $Le_1$ ,  $Le_2$ ,  $Nc_1$ ,  $Nc_2$  and  $Ra$ . The Rayleigh number for the natural convection in the porous medium is considered in the practical range of  $Ra < 100$ . The Lewis number for gas mixtures is less than unity (i.e., Lewis number of the moisture air is about 0.8) and for some liquid mixtures is higher than unity. Hence, the Lewis number is considered in the range of 0.1–10. In the study of Costa (2004),

**Table 3** The evaluated values of  $Nu$ ,  $Sh_1$  and  $Sh_2$  for different grid sizes when  $Le_2 = 0.8$ ,  $Nc_1 = 2.0$  and  $Nc_2 = 2.0$ 

Grid size	$Ra$	$Le_1$	$Nu$			$Sh_1$			$Sh_2/Le_2$		
			$50 \times 50$	$100 \times 100$	$150 \times 150$	$50 \times 50$	$100 \times 100$	$150 \times 150$	$50 \times 50$	$100 \times 100$	$150 \times 150$
50	0.1		5.968	5.968	5.968	1.205	1.205	1.205	5.105	5.105	5.105
	1		5.836	5.836	5.835	5.836	5.835	5.835	4.862	4.862	4.862
	10		4.717	4.716	4.716	22.409	22.408	2.2408	3.867	3.867	3.867
100	0.1		9.100	9.099	9.099	1.521	1.520	1.520	7.887	7.887	7.887
	1		9.080	9.079	9.079	9.079	9.079	9.079	7.653	7.652	7.652
	10		7.462	7.462	7.462	33.183	33.182	33.182	6.169	6.168	6.168



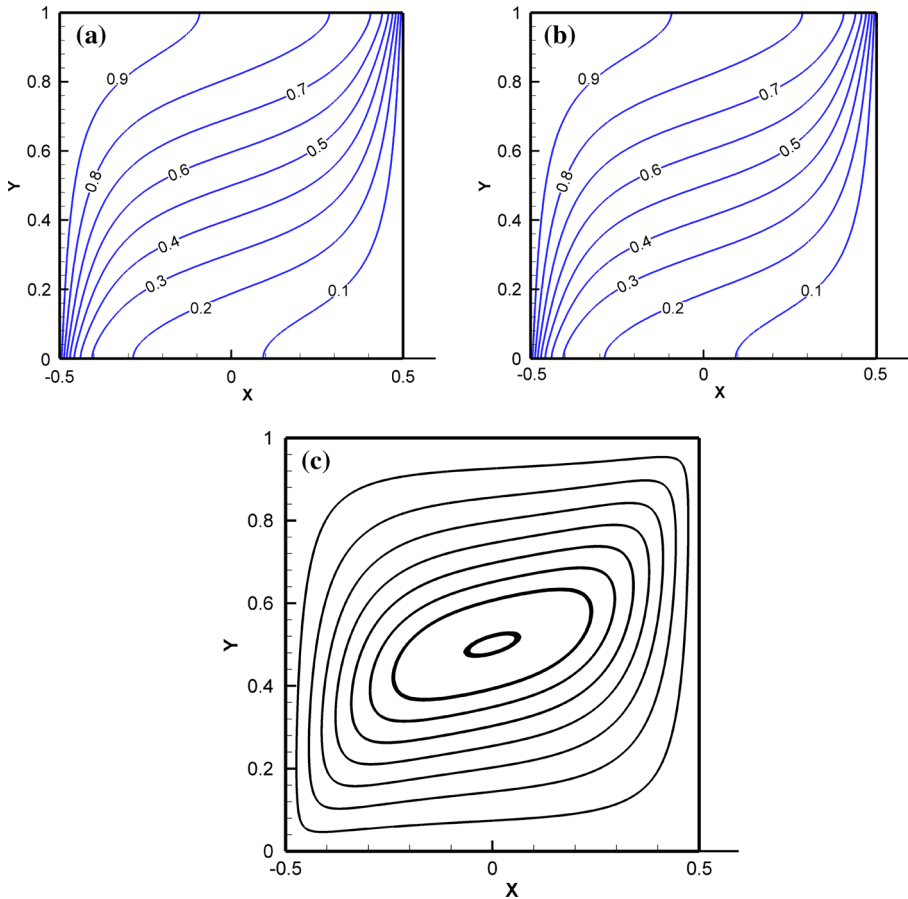


**Fig. 2** The isotherms, isoconcentrations and the streamlines for  $Le_1 = Le_2 = 0.8$ ,  $Nc_1 = Nc_2 = 2.0$  and  $Ra = 25$ . **a** Isotherms ( $\theta$ ). **b** Isoconcentrations ( $\phi_1$ ). **c** Streamlines ( $\psi$ )

the buoyancy ratio parameters are adopted in range of 0–5. Here, the range of buoyancy ratio parameters,  $Nc_1$  and  $Nc_2$ , is adopted between 0 and 10.

Figures 2 and 3 show the contours of the isotherms, concentration of phase 1 and the streamlines for  $Ra = 25$  and  $Ra = 100$ , respectively. The results of these figures are reported for fixed value of  $Le_1 = Le_2 = 0.8$ ,  $Nc_1 = Nc_2 = 2.0$ . As the values of Lewis number and the buoyancy ratio parameters for two phases are equal, the contours of concentration for both phases of 1 and 2 are identical in this case. Comparison between the results of Figs. 2 and 3 shows that the increase in the Rayleigh number increases the velocity of the flow in the vicinity of the walls, and hence, the isotherms and isoconcentrations are closer to the walls for the case of  $Ra = 100$ . In the case of  $Ra = 100$ , the heat and mass transfer in the core of the cavity is almost vertical due to diffusion.

Figure 4 shows the isotherms, streamlines and isoconcentrations for phases of 1 and 2 for the case of  $Le_1 = 0.8$ ,  $Le_2 = 10.0$ ,  $Nc_1 = 2.0$ ,  $Nc_2 = 10.0$  and  $Ra = 100$ . Indeed, the increase in  $Le_2$  tends to decrease the thickness of the concentration boundary layer, formed near the walls. The increase in  $Nc_2$  also tends to increase the induced buoyancy effects due

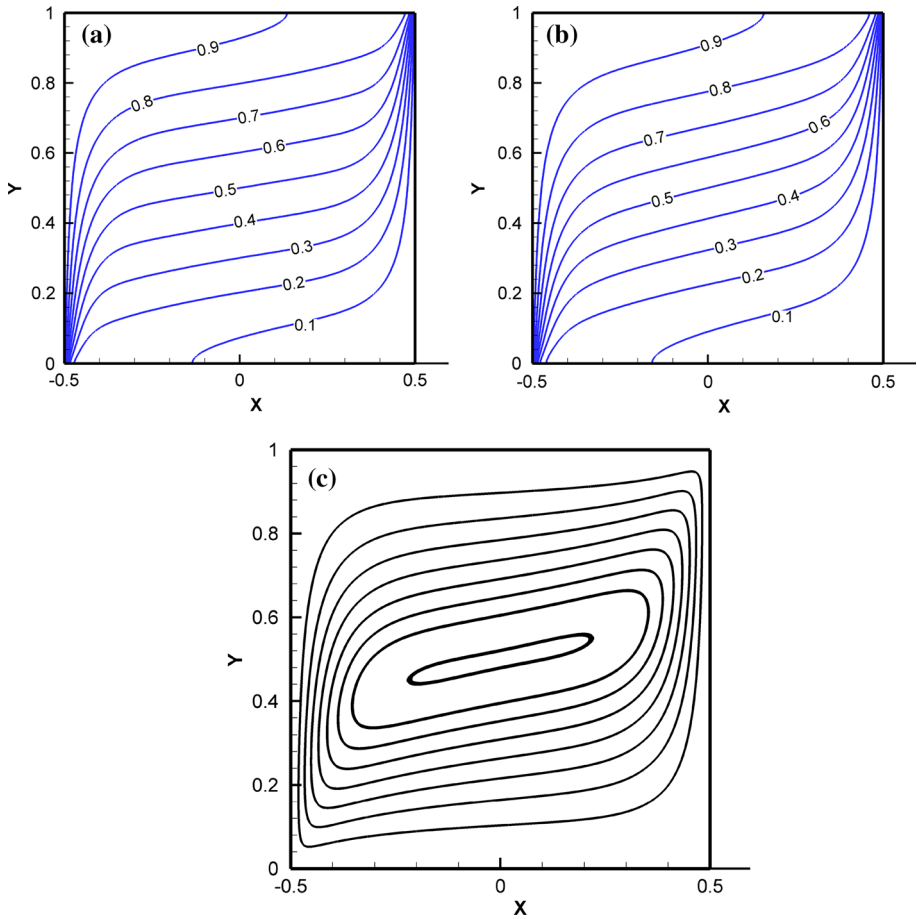


**Fig. 3** The isotherms, isoconcentration and the streamlines for  $Le_1 = Le_2 = 0.8$ ,  $Nc_1 = Nc_2 = 2.0$  and  $Ra = 100$ . **a** Isotherms ( $\theta$ ). **b** Isoconcentrations ( $\phi_1$ ). **c** Streamlines ( $\psi$ )

to mass transfer. The  $Nc_2$  higher than unity indicates that the buoyancy effects due to mass transfer of phase 2 are strong and comparable with the thermal buoyancy effects. Hence, the migration of phase 2 in the vicinity of the vertical walls strongly influences the streamlines and the effect of mass transfer of phase 2 is the dominant effect in the cavity. In contrast with streamlines of Fig. 2c, which almost follow the isotherm patterns, the streamlines of Fig. 3b are under the influence of the concentration of phase 2. The mass transfer of phase 2 in the middle of the cavity is diffusive dominant and in vertical direction.

Comparison between the results of this figure and Fig. 2 indicates that the isotherms and isoconcentrations of phase 1 are compacted in the bottom left and top right corners of the cavity. This is because of the increase in the velocity of the fluid near the vertical walls because of the induced strong buoyancy forces of phase 2. Almost entire of the top of the cavity is hot and high concentration of phase 1, and entire of the bottom of the cavity is cold and low concentration of phase 1. Hence, the temperature and concentration boundary layers next to the vertical walls almost follow the patterns of the streamlines, induced by the phase 1.

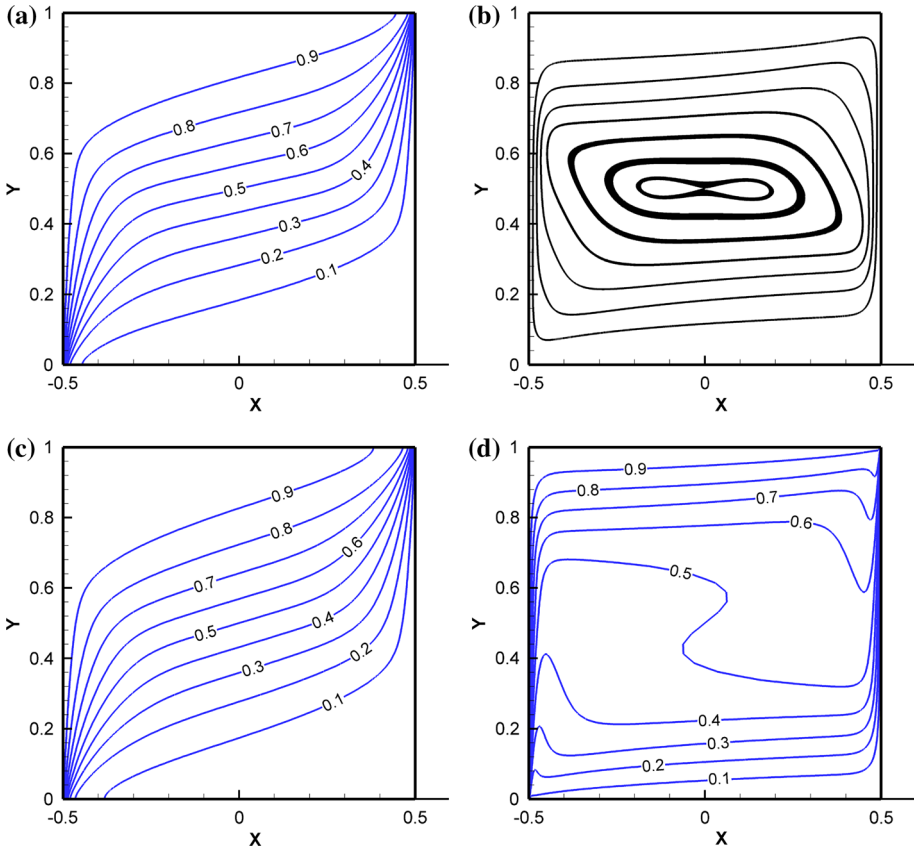


**Fig. 4** The isotherms, streamlines and isoconcentrations for  $Le_1 = 0.8, Le_2 = 10.0, N_{c1} = 2.0, N_{c2} = 10.0$  and  $Ra = 100$ . **a** Isotherms ( $\theta$ ). **b** Streamlines ( $\psi$ ). **c** Isoconcentrations ( $\phi_1$ ). **d** Isoconcentrations ( $\phi_2$ )

Figures 5, 6 and 7 show the average Nusselt number for mixture (fluid), the average Sherwood number for phase 1 and the average Nusselt number for phase 2, respectively. The parameters of interest, i.e.,  $Nu, Sh_1$  and  $Sh_2$ , are plotted as a function of Lewis number for phase 1 ( $Le_1$ ) and for various values of the Lewis number for phase 2 ( $Le_2$ ). Figure 5 shows that for very small values of  $Le_1$ , the Nusselt number increases and then starts to decrease monotonically. Hence, for small values of  $Le_1$  (about 0.1) there are maximum values for Nusselt number. The increase in  $Le_1$  tends to reduce the thickness of the concentration boundary layer next to the wall. Figure 7 also shows a peak for the mass transfer of phase 2 at the surface ( $Sh_2$ ) about  $Le_1 = 0.1$  for small value of  $Le_2$  ( $Le_2 = 1, Le_2 = 2.0$ ). However, for large value of  $Le_2$ , i.e.,  $Le_2 = 10.0$ , the observed peak is very smooth and shifts to values of  $Le_1 \approx 2$ . These figures also depict that the increase in  $Le_1$  or  $Le_2$  reduces the Nusselt number. As shown in Fig. 4, for large values of Lewis number, the thickness of the formed boundary layer of concentration over the vertical walls decreases.

For very large values of Lewis numbers, the concentration gradient over the vertical walls is a very narrow region next to the walls, in which the induced buoyancy effect due to concentration gradient is very strong. In the mentioned narrow regions, the flow would move fast toward the top (for hot and high concentration) and toward bottom (for cold and low

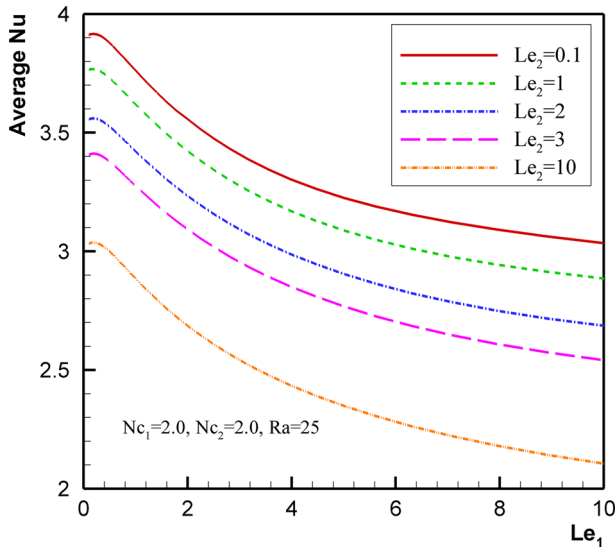


**Fig. 5** The variation of average Nusselt number as a function of  $Le_1$  for various values of  $Le_2$

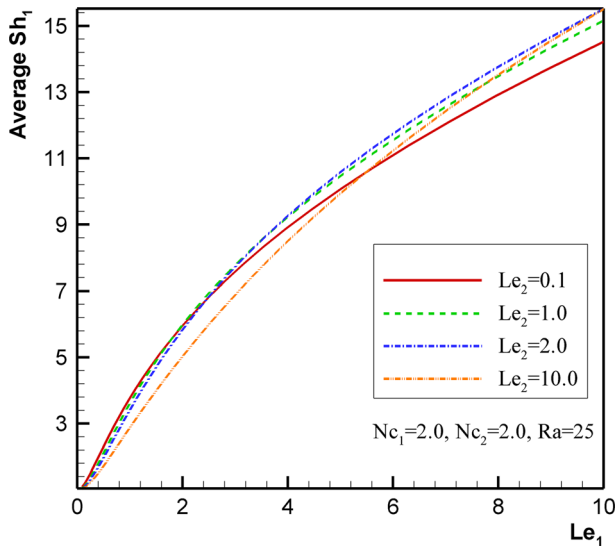


**Fig. 6** The variation of average Sherwood number for phase 1 as a function of  $Le_1$  for various values of  $Le_2$

concentration) walls. The strong flow near the vertical walls will carry a significant amount of the volume fraction of the corresponding phase and a lower amount of the other phase from the area adjacent to vertical walls and move it toward the horizontal top and bottom walls.

It should be noticed that in the regions next to walls, where the flow is fast, Darcy's forces are also very large and tend to reduce the velocities at the edge of the boundary layers instantly. Hence, the rest of the cavity is almost stratified. In the stratified regions, the mass transfer is mostly limited to the diffusive mechanism. Indeed, as the Lewis numbers increases, the

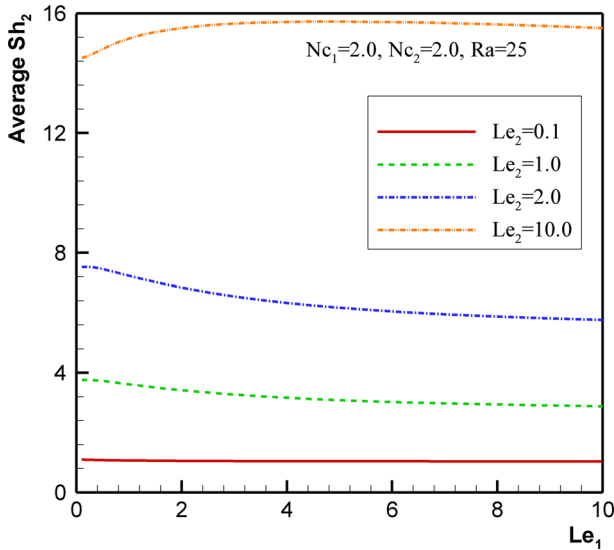


**Fig. 7** The variation of average Sherwood number for phase 2 as a function of  $Le_1$  for various values of  $Le_2$

induced buoyancy forces, due to mass transfer effects, are strong, but the effective regions are very limited. When the Lewis number decreases, the thickness of the boundary layer increases, and hence, the buoyancy force due to mass transfer could be distributed in a larger area; as a result, the induced velocities in the cavity are smooth. When the Lewis number significantly decreases, the affective region of the buoyancy induced force due to mass transfer reaches the core of the cavity. Increasing the Lewis number beyond this point would reduce the induced mass transfer buoyancy force in the entire cavity, and consequently, it would reduce the flow velocities, the Sherwood and Nusselt numbers, which this is the reason for the observed maximum Sherwood and Nusselt peaks in Figs. 5 and 7.

Figures 6 and 7 show that the increase in the Lewis number for phase 1 would increase the Sherwood for phase 1 ( $Sh_1$ ), and similarly the increase in  $Le_2$  increases  $Sh_2$ . As mentioned, the increase in  $Le$  decreases the thickness of the concentration boundary layer over the vertical walls for the corresponding phase, which results in the augmentation of the concentration slope (Sherwood number) of the corresponding phase at the vertical walls. The effect of variation of Lewis number for a phase is complicated on the other phase. Figure 7 shows some peaks for  $Sh_2$  by the variation of the  $Le_1$ . The reason for these peaks is similar to those for Nusselt number in Fig. 5.

Figures 8, 9 and 10 show the average Nusselt number for the mixture, the average Sherwood number for phase 1 and the average Sherwood number for phase 2, respectively. These figures depict the effect of the buoyancy ratio parameters ( $Nc_1$  and  $Nc_2$ ) as a function of the Lewis number for phase 1 ( $Le_1$ ) on the heat and mass transfer in the cavity. These figures also in agreement with the previous figures depict the maximum peaks for the average Nusselt number and the average Sherwood number for phase 2.

Figure 8 shows that the increase in buoyancy ratio parameters increases the average Nusselt number. Indeed, the induced buoyancy force due to mass transfer is a function of the Lewis number and the corresponding buoyancy ratio parameter. The Lewis number dictates the affecting area of the buoyancy force and the corresponding buoyancy ratio parameter dictates the strength of the induced buoyancy force. For each phase, the variation of these sets of

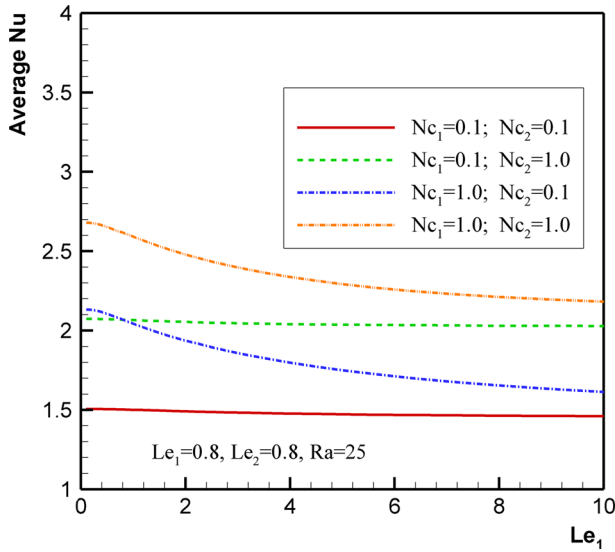


**Fig. 8** The variation of average Nusselt number as a function of  $Le_1$  for different values of the buoyancy ratio parameters of  $Nc_1$  and  $Nc_2$

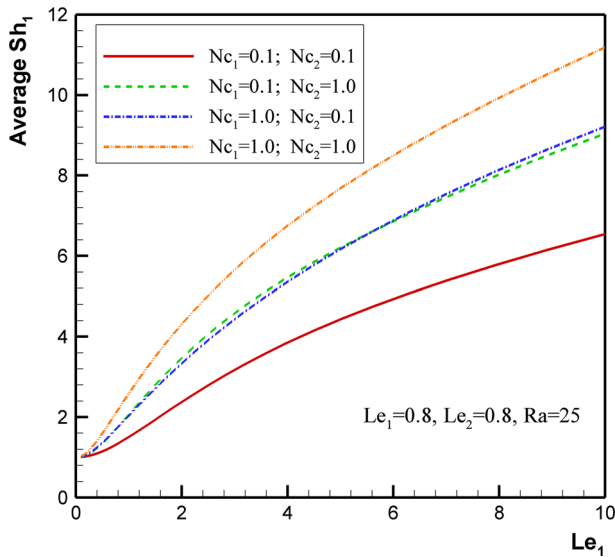


**Fig. 9** The variation of average Sherwood number for phase 1 as a function of  $Le_1$  for different values of the buoyancy ratio parameters of  $Nc_1$  and  $Nc_2$

parameters (i.e.,  $Le$  and  $Nc$ ) would directly affect the flow and then the heat transfer rate from the surface. However, the variation of these parameters ( $Le$  and its corresponding  $Nc$ ) would indirectly affect the other phase through the effect on the streamlines. Hence, the green dash line indicates that the raise of  $Nc_2$  increases the average Nusselt number; however, this increase is almost independent of the Lewis number for phase 1 ( $Le_1$ ). The blue dash-dot line indicates that the raise of  $Nc_1$  also increases average Nusselt number, but the observed

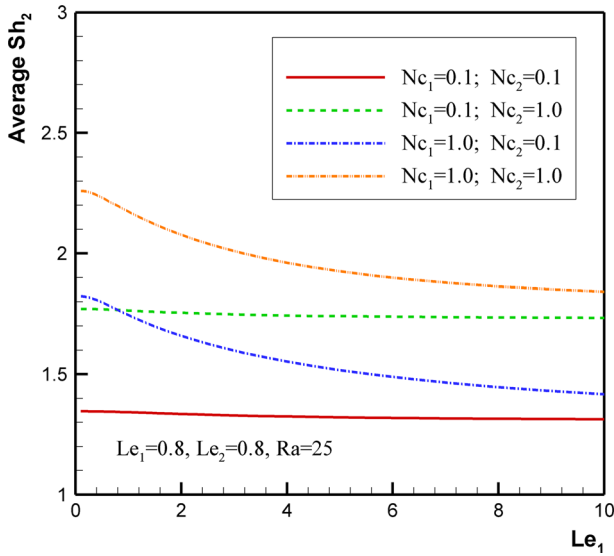


**Fig. 10** The variation of average Sherwood number for phase 2 as a function of  $Le_1$  for different values of the buoyancy ratio parameters of  $N_{c_1}$  and  $N_{c_2}$

increase is a decreasing function of the  $Le_1$ . Comparison between the dashed line (green line for  $N_{c_1} = 0.1$  and  $N_{c_2} = 1.0$ ) and the dash-dot line (blue line for  $N_{c_1} = 1.0$  and  $N_{c_2} = 0.1$ ) in Fig. 8 indicates that the effective region of phase 1 is wide when the  $Le_1$  is very small, and hence, the increase in  $N_{c_1}$  from 0.1 to 1.0 induces high and smoother buoyancy forces, and consequently, it results in higher values of average Nusselt number compared to the same increase in the amount of  $N_{c_2}$ . The same conclusion as Fig. 8 is also true for Fig. 10 as the second phase would also follow the induced flow patterns as the temperature distribution in the cavity. Figures 8, 9 and 10 show that the increase in  $Le_1$  raises the average mass transfer for its corresponding phase (average Sherwood number for phase 1). The raise of  $N_{c_1}$  or  $N_{c_2}$  would boost the heat and mass transfer from the surface due to the enhancement in the buoyancy forces.

Figures 11 and 12 show the effect of buoyancy ratios ( $N_{c_1}$ ) and ( $N_{c_2}$ ) on the average Nusselt number and the average Sherwood number of phase 1, when  $Le_1 = Le_2 = 0.8$ . Figures 11 and 12 in agreement with Figs. 8, 9 and 10 show that the increase in the buoyancy ratio parameters increases the heat and mass transfer from the surface. These figures indicate that the increase in the average Nusselt and Sherwood numbers is almost a linear function of the buoyancy ratios. As the Lewis number for both phases is considered equal ( $Le_1 = Le_2 = 0.8$ ), the obtained Sherwood numbers for both phases would be the same, and hence, the figure of  $Sh_2$  is not depicted here for the sake of brevity.

Figures 13, 14 and 15 show the average Nusselt number for the mixture, the average Sherwood number for phase 1 and the average Sherwood number for phase 2, respectively. These figures depict the effect of the Rayleigh number as a function of the  $Le_1$  on the heat and mass transfer in the cavity. These figures illustrate that the increase in the Rayleigh number boosts the heat and mass transfer from the surfaces. The increase in Rayleigh number almost linearly shifts the Nusselt number curves upwards. When Lewis number is about unity, the thickness of the concentration boundary layer is about the thickness of the temperature boundary layer over the vertical and horizontal walls, and hence, the behaviors of the temperature distrib-

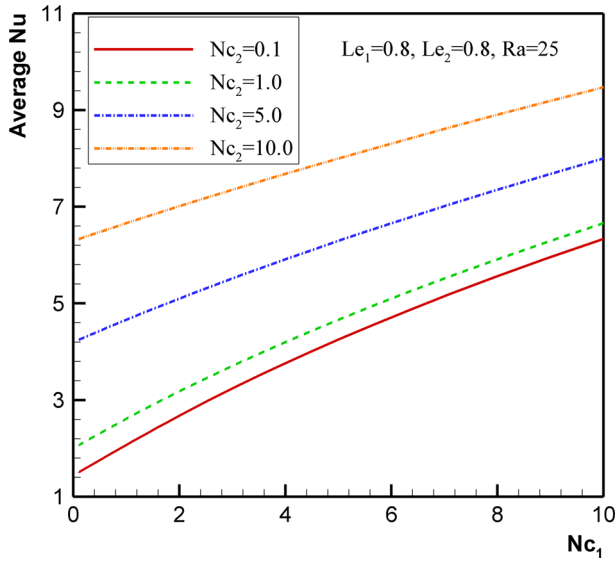


**Fig. 11** The variation of average Nusselt number as a function of  $Le_1$  for different values of the buoyancy ratio parameters of  $Nc_1$  and  $Nc_2$

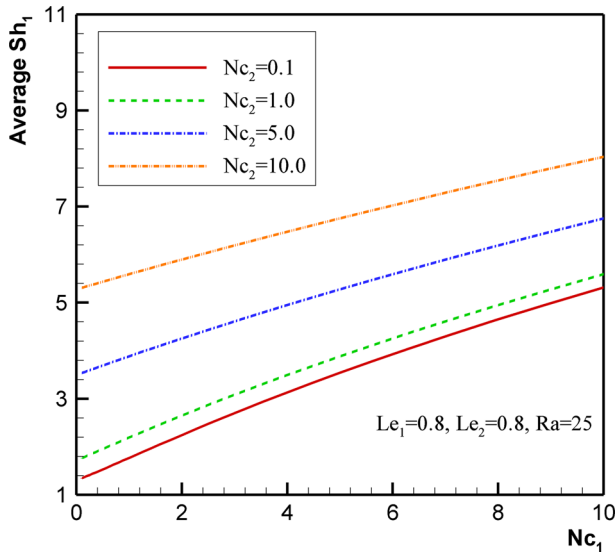


**Fig. 12** The variation of average Sherwood number for phase 1 as a function of  $Le_1$  for different values of the buoyancy ratio parameters of  $Nc_1$  and  $Nc_2$

ution in the cavity are very similar to the concentration distribution for this phase. Thus, in Fig. 15, in which  $Le_2 = 0.8$  (about unity) the pattern and the order of magnitude of Nusselt and Sherwood numbers ( $Nu$  and  $Sh_2$ ) are very similar. This is because of the fact that the variation of  $Le_1$  indirectly and through the streamlines affects  $Nu$  and  $Sh_2$ .



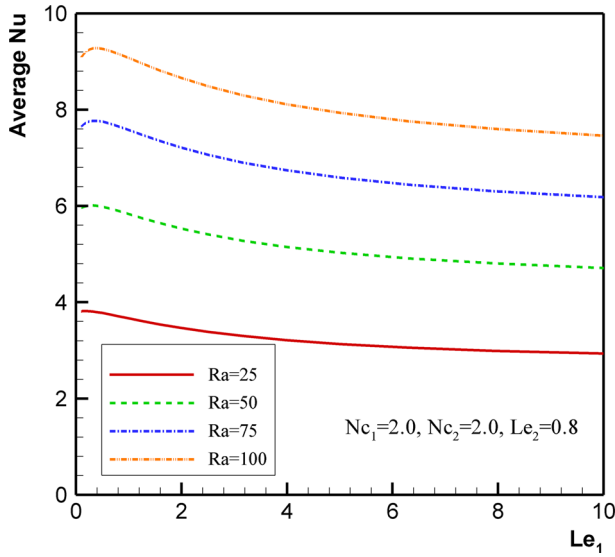


**Fig. 13** The variation of average Nusselt number as a function of  $Le_1$  for different values of the Rayleigh number

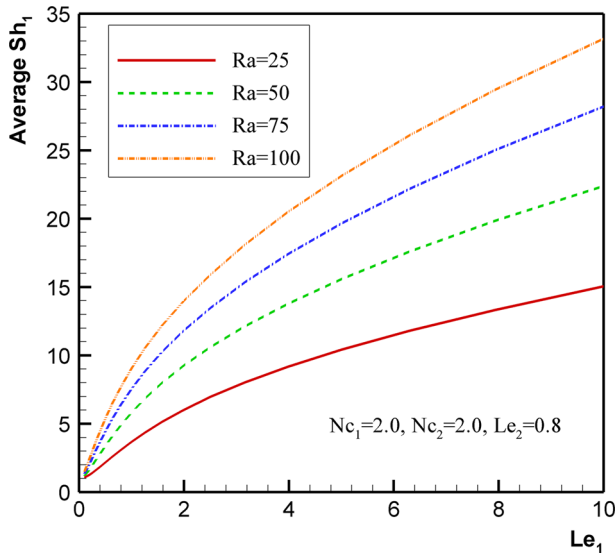


**Fig. 14** The variation of average Sherwood number for phase 1 as a function of  $Le_1$  for different values of the Rayleigh number

For very small values of Rayleigh number, the induced buoyancy forces due to heat and mass transfer are small, and hence, the variation of Lewis or buoyancy ratio only shows smooth effects on the heat and mass transfer parameters (i.e.,  $Nu$  and  $Sh$ ). The raise of the Rayleigh number boosts the effect of  $Nc$  and  $Le$  and induces large buoyancy forces. As a result, the increase in Rayleigh number increases the effect of the variation of Lewis number on the mass transfer from the walls (see Fig. 14).

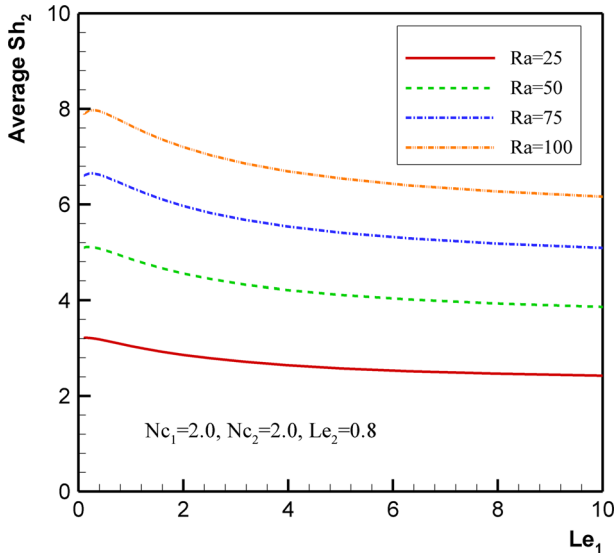


**Fig. 15** The variation of average Sherwood number for phase 2 as a function of  $Le_1$  for different values of the Rayleigh number

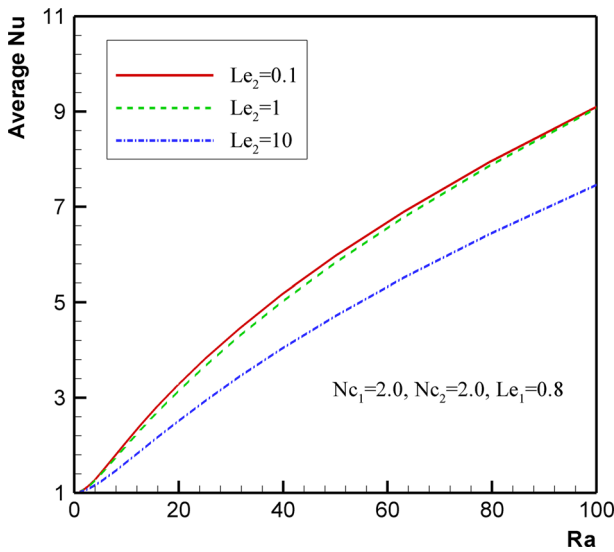


**Fig. 16** The variation of average Nusselt number as a function of Rayleigh number for different values of Lewis number of phase 2

Figures 16, 17 and 18 show the average Nusselt number for the mixture, the average Sherwood number for phase 1 and the average Sherwood number for phase 2, respectively, as a function of Rayleigh number and various values of  $Le_2$ . These figures also depict that the average Nusselt number and average Sherwood number for phase 1 are a raising function of the Rayleigh number but a decreasing function of  $Le_2$ . The variation of Rayleigh number and Lewis number ( $Le_2$ ) in Fig. 18 interestingly shows when the  $Le_2$  is very small ( $Le_2 = 0.1$ ), and the raise of Rayleigh number does not affect the mass transfer from the wall. For large

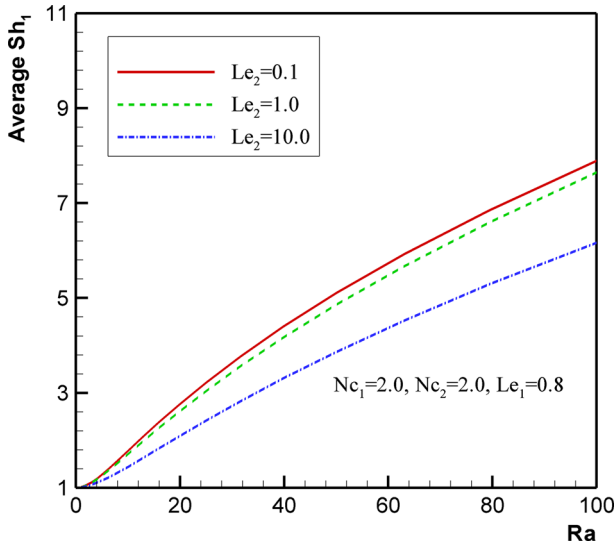


**Fig. 17** The variation of average Sherwood number for phase 1 as a function of Rayleigh number for different values of Lewis number of phase 2

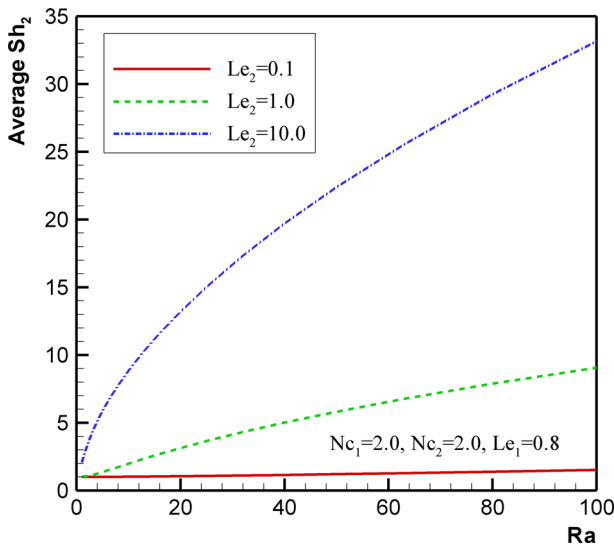


**Fig. 18** The variation of average Sherwood number for phase 2 as a function of Rayleigh number for different values of Lewis number of phase 2

values of Rayleigh number, the increase in Rayleigh number significantly increases the mass transfer from the wall ( $Sh_2$ ). The large values of  $Le_2$  result in a very narrow boundary layer of concentration for phase 2 and large gradients of the concentration for phase 2. The buoyancy forces are also strong in the mentioned narrow region. Hence, in this case, any increase in the Rayleigh number significantly boosts the mass transfer for phase 2. In contrast, when the  $Le_2$  is very small, the concentration gradients, and the corresponding buoyancy forces are very low and the increase in Rayleigh number could only show very smooth effects on  $Sh_2$ .

## 5 Conclusion

Triple-diffusive natural convection flow, heat and mass transfer of a mixture in a square porous cavity is theoretically analyzed. The governing partial differential equations were transformed into a non-dimensional form. The non-dimensional governing equations are a function of Rayleigh number, Lewis numbers for phases 1 and 2, and the buoyancy ratios for phases 1 and 2. The governing equations were solved using a finite element code. The effect of the non-dimensional parameters on the flow, temperature and concentrations was studied. The main outcomes of the present study can be summarized as follows:

- (1) When the Lewis number of a phase is about 0.1, there is a maximum value for the heat transfer and mass transfer of the other phase due to strong mass transfer buoyancy forces.
- (2) The increase in Lewis number increases the mass transfer of the corresponding phase from the wall, but it could reduce or raise the mass transfer of the other phase, depending on the Lewis number of the second phase.
- (3) The increase in the buoyancy ratio parameters and the Rayleigh number boosts the mass transfer buoyancy forces and increases the heat and mass transfer.
- (4) When the Lewis number for a phase is small, the augmentation of Rayleigh number cannot induce a significant boost on the mass transfer of the corresponding phase.

In the present study, as a first study, we focused on the aided mass transfer of the phases. The future studies can focus on the opposing mass transfer on the triple-convective heat transfer. In addition, it was found that the mass transfer of a phase could significantly affect the heat transfer of the mixture as well as the mass transfer of the other phase; hence, one of the phases could be employed as a controlling phase for control of heat and mass transfer in the system.

**Acknowledgments** This work of M.A. Sheremet was conducted as a government task of the Ministry of Education and Science of the Russian Federation, Project Number 13.1919.2014/K. M. Ghalambaz is thankful to Ahvaz Branch, Islamic Azad University, Ahvaz, Iran. The authors wish also to express their thanks to the very competent Reviewers for the very good comments and suggestions.

## References

- Abdou, M.M., Chamkha, A.J.: Double diffusion mixed convection in an axisymmetric stagnation flow of a nanofluid over a vertical cylinder. *Comput. Therm. Sci.* **4**, 201–212 (2012)
- Basak, T., Roy, S., Balakrishnan, A.R.: Effects of thermal boundary conditions on natural convection flows within a square cavity. *Int. J. Heat Mass Transf.* **49**, 4525–4535 (2006a)
- Basak, T., Roy, S., Paul, T., Pop, I.: Natural convection in a square cavity filled with a porous medium: effects of various thermal boundary conditions. *Int. J. Heat Mass Transf.* **49**, 1430–1441 (2006b)
- Baytas, A.C., Pop, I.: Free convection in oblique enclosures filled with a porous medium. *Int. J. Heat Mass Transf.* **42**, 1047–1057 (1999)
- Bulgarkova, N.S.: Condition of the onset and nonlinear regimes of convection of a three-component isothermal mixture in a porous rectangle under modulation of the concentration gradient. *Fluid Dyn.* **47**, 608–619 (2012)
- Beckermann, C., Viskanta, R., Ramadhyani, S.: A numerical study of non-Darcian natural convection in a vertical enclosure filled with a porous medium. *Numer. Heat Transf.* **10**, 446–469 (1986)
- Bejan, A.: On the boundary layer regime in a vertical enclosure filled with a porous medium. *Lett. Heat Mass Transf.* **6**, 82–91 (1979)
- Capone, F., De Luca, R.: Onset of convection for ternary fluid mixture saturating horizontal porous layer with large pores. *Att. Acad. Nat. Lince Classes ci. Fiz. Mat. Nat.* **23**, 405–428 (2012)

- Chamkha, A.J., El-Aminand, M.F., Aly, A.M.: Unsteady double-diffusive natural convective MHD flow along a vertical cylinder in the presence of chemical reaction, thermal radiation and Soret and Dufour effects. *J. Naval Archit. Mar. Eng.* **8**, 25–36 (2011)
- Chamkha, A.J., Al-Mudhaf, A.: Double-diffusive natural convection in inclined porous cavities with various aspect ratios and temperature-dependent heat source or sink. *Int. J. Heat Mass Transf.* **44**, 679–693 (2008)
- Chamkha, A.J., Mansour, M.A., Ahmad, S.E.: Double-diffusive natural convection in inclined finned triangular porous enclosures in the presence of heat generation/absorption effects. *Int. J. Heat Mass Transf.* **46**, 757–768 (2010)
- Chand, S.: Effect of rotation on triple-diffusive convection in a magnetized ferrofluid with internal angular momentum saturating a porous medium. *Appl. Math. Sci.* **6**, 3245–3258 (2012)
- Chand, S.: Linear stability of triple-diffusive convection in micropolar ferromagnetic fluid saturating porous medium. *Appl. Math. Mech.* **34**, 309–326 (2013)
- Costa, V.A.F.: Double-diffusive natural convection in parallelogrammic enclosures filled with fluid-saturated porous media. *Int. J. Heat Mass Transf.* **47**, 2699–2714 (2004)
- Gross, R., Bear, M.R., Hickox, C.E.: The application of flux-corrected transport (FCT) to high Rayleigh number natural convection in a porous medium. In: *Proceedings of the 7th International Heat Transfer Conference*, San Francisco, CA (1986)
- Ingham, D.B., Pop, I. (eds.): *Transport Phenomena in Porous Media III* (Vol. 3). Elsevier, London (2005)
- Kantur, O.Y., Tsubulin, V.G.: Numerical investigation of the plane problem of convection in a multicomponent fluid in a porous medium. *Fluid Dyn.* **39**, 464–473 (2004)
- Khan, W.A., Pop, I.: The Cheng–Minkowycz problem for triple-diffusive natural convection boundary layer flow past a vertical plate in a porous medium. *J. Porous Media* **16**, 637–646 (2013)
- Khan, Z.H., Khan, W.A., Pop, I.: Triple diffusive free convection along a horizontal plate in porous media saturated by a nanofluid with convective boundary condition. *Int. J. Heat Mass Transf.* **66**, 603–612 (2013)
- Khan, Z.H., Culham, J.R., Khan, W.A., Pop, I.: Triple convective-diffusion boundary layer along a vertical flat plate in a porous medium saturated by a water-based nanofluid. *Int. J. Therm. Sci.* **90**, 53–61 (2015)
- Mahdy, A., Chamkha, A.J., Baba, Y.: Double-diffusive convection with variable viscosity from a vertical truncated cone in porous media in the presence of magnetic field and radiation effects. *Comput. Math. Appl.* **59**, 3867–3878 (2010)
- Mallikarjuna, B., Chamkha, A.J., Vijaya, R.B.: Soret and dufour effects on double diffusive convective flow through a non-darcy porous medium in a cylindrical annular region in the presence of heat sources. *J. Porous Media* **17**, 623–636 (2014)
- Manole, D.M., Lage, J.L.: Numerical benchmark results for natural convection in a porous medium cavity. *Heat Mass Transf. Porous Media ASME Conf.* **105**, 44–59 (1992)
- Moya, S.L., Ramos, E., Sen, M.: Numerical study of natural convection in a tilted rectangular porous material. *Int. J. Heat Mass Transf.* **30**, 630–645 (1987)
- Poulikakos, D.: The effect of a third diffusing component on the onset of convection in a horizontal porous layer. *Phys. Fluids* **28**, 3172–3174 (1985)
- Ravikumar, V., Raju, M.C., Raju, G.S., Chamkha, A.J.: MHD double diffusive and chemically reactive flow through porous medium bounded by two vertical plates. *Int. J. Energy Technol.* **5**, 1–8 (2013)
- Reddy, J.N.: *An Introduction to the Finite Element Method*. McGraw-Hill, New York (1993)
- Rionero, S.: Absence of subcritical instabilities and global nonlinear stability for porous ternary diffusive-convective fluid mixtures. *Phys. Fluids* **24**, 104101 (2012)
- Rionero, S.: Triple diffusive convection in porous media. *Acta Mech.* **224**, 447–458 (2013)
- Rionero, S.: On the nonlinear stability of ternary porous media via only one necessary and sufficient algebraic condition. *Evol. Equ. Control Theory* **3**, 525–539 (2014)
- Rionero, S.: Influence of depth-dependent Brinkman viscosity on the onset of convection in ternary porous layers. *Transp. Porous Media* **106**, 221–236 (2015)
- Rudraiah, N., Vortmeyer, D.: The influence of permeability and of a third diffusing component upon the onset of convection in a porous medium. *Int. J. Heat Mass Transf.* **25**, 457–464 (1982)
- Subhashini, S.V., Samuel, N., Pop, I.: Double-diffusive convection from a permeable vertical surface under convective boundary condition. *Int. Commun. Heat Mass Transf.* **38**, 1183–1188 (2011)
- Varol, Y., Oztop, H.F., Pop, I.: Numerical analysis of natural convection for a porous rectangular enclosure with sinusoidally varying temperature profile on the bottom wall. *Int. Commun. Heat Mass Transf.* **35**, 56–64 (2008)
- Walker, K.L., Homsy, G.M.: Convection in a porous cavity. *J. Fluid Mech.* **87**, 338–363 (1978)